2. Ray WA, Chung CP, Stein CM, et al. Association of rivaroxaban vs apixaban with major ischemic or hemorrhagic events in patients with atrial fibrillation. *JAMA*. 2021;326(23):2395-2404.
3. Ortel TL, Neumann I, Ageno W, et al. American Society of Hematology 2020 guidelines for management of venous thromboembolism: treatment of deep vein thrombosis and pulmonary embolism. *Blood Adv*. 2020;4(19):4693-4738.
4. Kearon C, Akl EA, Ornelas J, et al. Antithrombotic therapy for VTE disease: CHEST guideline and expert panel report. *Chest*. 2016;149(2):315-352.

SUPPORTING INFORMATION

Additional supporting information may be found in the online version of the article at the publisher's website.

Received: 20 January 2022 | Revised: 8 February 2022 | Accepted: 10 February 2022

DOI: 10.1002/ajh.26502

Prediction of outcomes in chronic lymphocytic leukemia patients treated with ibrutinib: Validation of current prognostic models and development of a simplified three-factor model

To the Editor:

The current shift in the treatment paradigm from chemoimmunotherapy (CIT) to targeted therapy complicates outcome prediction in chronic lymphocytic leukemia (CLL).[1] Existing prognostic markers have assumed new meanings in this treatment transition, while others have become less relevant or even obsolete.[2–4] Likewise, prognostic models developed during the CIT era, namely the CLL International Prognostic Index (CLL-IPI), and Barcelona-Brno (B-B) score, have lost part of their predictive power in the era of targeted therapy.[5–7]

Nowadays, ibrutinib, the first-in-class Bruton kinase (BTK) inhibitor, may claim the most extensive use in clinical practice compared to other targeted agents.[8] However, the magnitude of improvement in progression-free survival (PFS) with ibrutinib depends on the patient subgroup.[3,4,9,10] As a result, clinicians need reliable tools to predict outcomes in this homogeneously treated patient subset.

Two prognostic models originating from pooled analyses of randomized clinical trials of ibrutinib, idelalisib, or venetoclax have recently been developed to predict the prognosis of patients treated with new drugs in the upfront or relapsed/refractory setting.[11,12] These four-factor models share standard variables, such as serum β_2-microglobulin and lactate dehydrogenase (LDH). Moreover, the model by Soumerai et al.[11] (formally indicated as the BALL score: β_2_microglobulin, Anemia, LDH, time from the Last therapy) is complemented by hemoglobin concentration and time from the start of last therapy, whereas the model by Ahn et al.[12,13] (formally indicated as CLL4 model) is complemented by prior treatment and *TP53* status.

These prognostic models provide a "globally applicable" approach for clinical use in patients treated with targeted agents; however, a comparative performance analysis possibly extended to models generated in the CIT era is lacking.

We analyzed a national multicenter patient cohort consisting of 338 CLL patients treated at 16 Italian hematological institutions outside the context of clinical trials between February 2013 and February 2019 with ibrutinib-based treatment. Of note, none of these patients had previously received venetoclax, idelalisib or other novel agents prior to ibrutinib. In this patient cohort, we assessed the reliability of four well-known prognostic CLL models (the CLL-IPI, B-B, BALL, and CLL4 scores) to predict patient clinical outcomes. Relevant endpoints, such as PFS and overall survival (OS) rates, were analyzed in terms of discriminatory power (such as c-Harrell), and relative goodness of fit was assessed using Akaike information criteria ([AIC] lower is better). PFS was defined as the time from ibrutinib starting to disease progression or death for any cause. Ibrutinib-related lymphocytosis was not considered progressive disease (PD) if in the setting of improvement in other disease parameters. Finally, a multivariate analysis allowed the identification of prognostically independent factors potentially useful for building a simplified three-factor model.

The median age of patients was 69 years (range 32–88), and 62% were males. A cumulative illness rating scale (CIRS) score >6 (range 0–16) was present in 57.4% of patients. Two-hundred and seventy (79.8%) patients had been previously treated (median number of prior therapies 2; range, 1–9) while 68 (20.1%) were treatment-naive. According to the baseline characteristics, 173 (51.1%) patients were in Rai stage III–IV, 148 (43.8%) had LDH values greater than upper normal limit (UNL) and 119 (35.2%) had β_2-miroglobulin values >5 mg/L. High-risk CLL was distributed over several defined features: (i) 11q deletion in 16.9% of patients, (ii) *TP53* aberrations in 50.3%, and (iii) unmutated immunoglobulin heavy chain (*IGHV*) gene status in 72.5%. Finally, early progression of disease (POD), defined as the time from the start of last therapy <24 months, was recorded in 228 (67.5%) patients (Table S1).

After a median follow-up of 36 months (range 4–85), 80 patients (23.6%) died, while 115 (34.0%) patients had a PFS event. One-hundred and fifty-one (44.6%) patients discontinued treatment. The most common reasons for ibrutinib discontinuation were PD (72/151, 47.6%), and adverse events (59/151, 39.0%). PD was evidenced as Richter's transformation (RT) in 17 patients (5.0%). In 26 patients (17.2%), the cause of ibrutinib discontinuation was related to death.

The 3-year PFS and OS were 70.7% (95% confidence interval [CI]: 65.6%–75.8%) and 78.1% (95% CI: 72.8%–83.4%), respectively. Risk scores developed in patients treated with targeted agents (CLL4 score and BALL) were applied to our cohort of patients and succeeded in predicting OS (Figure 1A,B; $p < .0001$ for both) and PFS (Figure 1C,D; $p < .0001$ for both). However, risk scores developed in patients treated

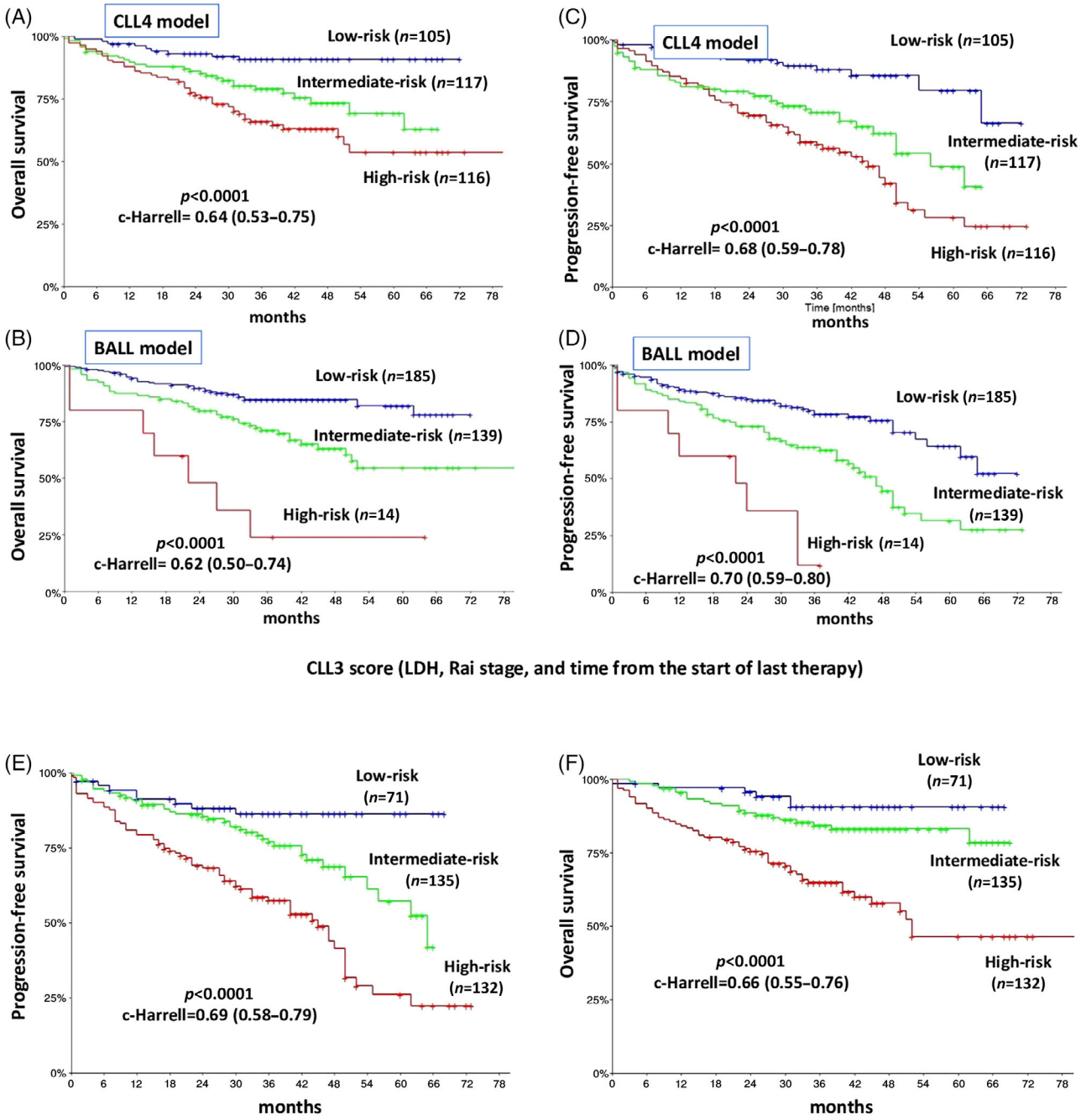

FIGURE 1 PFS and OS of 338 CLL patients receiving an ibrutinib-based therapy. OS analysis of patients stratified according to the CLL4 (A) and BALL (B) models. PFS of patients stratified according to the CLL4 (C), BALL (D) scores. PFS (E) and OS (F) of patients stratified according to a three-factor model (CLL3) (LDH, Rai stage, and time from the start of last therapy). The CLL3 score identifies three risk groups: (1) low risk with no factor, (2) intermediate risk with one factor, and (3) high risk with two or three factors. BALL (β2−microglobulin, Anemia, LDH, time from the Last therapy); CLL4 (TP53 aberration, prior treatment, β2-microglobulin ≥ 5 mg/L, and LDH > 250 U/L). CLL, chronic lymphocytic leukemia; LDH, lactate dehydrogenase; OS, overall survival; PFS, progression-free survival

with CIT (CLL-IPI and B-B score) worked only in the PFS prediction ($p = .002$ for B-B and $p = .01$ for CLL-IPI as shown in Figure S1A,B) but failed to predict OS ($p = .07$ for B-B and $p = .36$ for CLL-IPI as shown in Figure S1C,D). Furthermore, a comparative performance analysis focusing on OS confirmed the higher discriminatory capacity of the CLL4 (c-Harrell = 0.64 [0.53–0.75]) and BALL models (c-Harrell = 0.62 [0.50–0.74]) compared to the CLL-IPI (c-Harrell = 0.56 [0.44–0.67]) and B-B (c-Harrell = 0.57 [0.46–0.68]) models.

Univariate analysis including 14 baseline factors identified nine factors associated with an inferior PFS (namely, advanced Rai stage, $p = .001$; previous therapy, $p = .001$; *TP53* aberrations, $p = .003$; *IGHV* unmutated, $p = .031$;increased β_2-microglobulin levels,

$p < .0001$; early POD, $p < .0001$; LDH > UNL, $p = .001$; anemia, $p < .0001$; and creatinine clearance <70 mL/min, $p = .01$). All but two (*TP53* aberrations and *IGHV* unmutated status) of these factors were associated with OS in univariate analysis: advanced Rai stage, $p = .001$; previous therapy, $p = .001$; increased β_2-microglobulin levels, $p < .0001$; early POD, $p < .0001$; LDH > UNL, $p = .002$; anemia, $p = .01$; and creatinine clearance <70 mL/min ($p = .001$) as shown in Table S2.

Results from PFS and OS multivariate analyses are shown in Table S2. The three baseline factors that emerged as independently associated with inferior PFS and inferior OS were LDH values >UNL, Rai stage III/IV, and early POD. Noteworthy, PFS and OS probability decreased with each incremental unfavorable factor that was significant in the multivariate analysis ($p < .0001$) as shown in Figures S2 and S3. Factors that emerged significant in the multivariate analysis were used to build a score that enabled to identify three risk groups: (1) low-risk with no factor ($n = 71$, 21%) present at the start of ibrutinib, (2) intermediate-risk with one factor ($n = 135$, 39.9%), and (3) high-risk with two or three factors ($n = 132$, 39.0%).

We investigated the level of agreement between the three-factor model (CLL3 score) and the CLL4 or BALL models. Results of concordance analysis indicated a substantial agreement between the CLL3 score and the CLL4 model (weighted $k = -0.007$; $p = .81$) as shown in Table S3, while the same did not apply to the BALL model (weighted $k = 0.34$; $p < .0001$) as shown in Table S4. Of note, the CLL3 score and the CLL4 model captured a similar amount of high-risk patients (39% and 34.3%, respectively); in contrast, only 4.1% of patients fell into the high-risk category when classified according to the BALL score.

PFS and OS analyses indicated the excellent predictive power of the CLL3 model. The 3-year PFS rates for low-, intermediate-, and high-risk groups were 86.4%, 77%, and 57.6%, respectively ($p < .0001$; c-Harrell = 0.69 [0.58–0.79]) (Figure 1E), while the 3-year OS rates were 91%, 84%, and 65%, respectively ($p < .0001$; c-Harrell = 0.66 [0.55–0.76]) (Figure 1F).

Finally, a comparative performance analysis carried out according to the AIC criteria (AIC lower is better) confirmed the validity of our model's relative goodness of fit in the OS prediction. Values of AIC were better for the CLL3 score (AIC, 851.2), with no apparent difference between the BALL (AIC, 856.7) and the CLL4 (AIC, 858.2) scores. In contrast, a PFS comparative performance analysis indicated that the CLL4 score (AIC, 928.0) fared better than the CLL3 (AIC, 934.6) and BALL (AIC, 936.2) scores, respectively (Table S5).

This study confirms the substantial failure of the CLL-IPI and B-B scores to assess OS in CLL patients homogeneously treated with ibrutinib. In contrast, both the BALL and CLL4 models provided a satisfactory risk stratification with regard to OS and PFS in this multicenter retrospective cohort of patients, endorsing their applicability in the clinical management and counseling of CLL patients treated with ibrutinib in the daily practice.

Although CLL4 and BALL scores revealed optimal discrimination power in development studies, their performance in this validation analysis is less remarkable.[11,12] This finding is primarily due to differences between our patient cohort (i.e., only cases treated with ibrutinib outside of clinical trials) and the patient cohort used to develop the BALL (i.e., cases treated with CIT or with novel agents such as ibrutinib, idelalisib, or venetoclax in six randomized clinical trials or managed at the Mayo Clinic) or CLL4 score (i.e., patients treated with ibrutinib in phase II and III trials). Of note, also with the new CLL3 score proposed here the *C*-statistic threshold of 0.70 was only approached (0.69 for PFS and 0.66 for OS). Finally, it is worth noting that the patient cohort utilized to build this three-factor model only contained a small proportion of CLL patients who were treated with ibrutinib in the upfront. This is a limitation of the CLL3 score's capacity to predict the clinical outcome of patients treated with ibrutinib as first-line therapy.

Compared to the CLL4 model, the CLL3 score does not include *TP53* aberrations which still retains its predictive power in the target therapy era.[14,15] Of note, CLL3 provided a reliable risk stratification of patients bearing ($n = 170$) (Figures S4A and S3B) or not ($n = 168$) *TP53* mutations (Figure S5A,B).

In conclusion, we are aware that there is room to improve the quality of reporting and analysis in both prognostic model development and external validation studies. We expect also that novel prognostic models might consider specific mechanisms of CLL progression and the risk of RT, one of the most severe complications associated with CLL.[1]

CONFLICT OF INTERESTS

SM received honoraria from Janssen, Abbvie, and AstraZeneca, advisory board for Janssen, Abbvie, and AstraZeneca. AV received honoraria from Janssen, Abbvie, CSL Behring, Italfarmaco. LT received research funding from Gilead, Roche, Janssen and Takeda, advisory board for Roche, Takeda, Abbvie, AstraZeneca. GMR received research funding from Gilead. FRM advisory board for Janssen, Takeda, and Abbvie. An Cu advisory board and speaker bureau for Roche, Abbvie, Gilead, and Janssen. RF advisory board and speaker bureau for Roche, Abbvie, Celgene, Incyte, Amgen, Janssen, Gilead, and Novartis. LL received honoraria from Abbvie, Janssen, Astra Zeneca, Beigene.

AUTHOR CONTRIBUTIONS

Stefano Molica and Francesca Romana Mauro designed the study. Stefano Molica wrote the paper and interpreted the data. Diana Giannarelli was responsible for statistical analysis. Andrea Visentin, Gianluigi Reda, Paolo Sportoletti, Anna Maria Frustaci, Annalisa Chiarenza, Stefania Ciolli, Candida Vitale, Luca Laurenti, Lorenzo De Paoli, Roberta Murru, Massimo Gentile, Riccardo Moia, Gian Matteo Rigolin, Luciano Levato, Annamaria Giordano, Giovanni Del Poeta, Caterina Stelitano, Marina Deodato, Claudia Ielo, Alessandro Noto, Valerio Guarente, Marta Coscia, Alessandra Tedeschi, Gianluca Gaidano, Antonio Cuneo, Livio Trentin recruited patients for this observational study and participated in the management of patient care. Robin Foà provided initial advices. All authors approved the manuscript.

DATA AVAILABILITY STATEMENT

The data that support the findings of this study are available from the corresponding author upon reasonable request.

Stefano Molica[1], Diana Giannarelli[2], Andrea Visentin[3], Gianluigi Reda[4], Paolo Sportoletti[5], Anna Maria Frustaci[6], Annalisa Chiarenza[7], Stefania Ciolli[8], Candida Vitale[9], Luca Laurenti[10], Lorenzo De Paoli[11], Roberta Murru[12], Massimo Gentile[13], Riccardo Moia[11], Gian Matteo Rigolin[14], Luciano Levato[1], Annamaria Giordano[15], Giovanni Del Poeta[16], Caterina Stelitano[17], Marina Deodato[6], Claudia Ielo[18], Alessandro Noto[4], Valerio Guarente[5], Marta Coscia[9], Alessandra Tedeschi[6], Gianluca Gaidano[11], Antonio Cuneo[14], Robin Foa'[18], Livio Trentin[3], Francesca Romana Mauro[18]

[1]*Department of Hematology-Oncology, Azienda Ospedaliera Pugliese-Ciaccio, Catanzaro, Italy*

[2]*Biostatistic Unit, Fondazione Policlinico Universitario A. Gemelli IRCCS, Rome, Italy*

[3]*Hematology and Clinical Immunology Unit, Department of Medicine, University of Padua, Padua, Italy*

[4]*Fondazione IRCCS Cà Granda Ospedale Maggiore Policlinico, Milan, Italy*

[5]*Institute of Hematology-Centro di Ricerca Emato-Oncologica (CREO), Department of Medicine, University of Perugia, Perugia, Italy*

[6]*Department of Hematology, Niguarda Cancer Center, ASST Grande Ospedale Metropolitano Niguarda Milano, Milan, Italy*

[7]*Division of Hematology, Ferrarotto Hospital, Catania, Italy*

[8]*Hematology Unit, Careggi Hospital, Florence, Italy*

[9]*Division of Hematology, A.O.U. Città della Salute e della Scienza di Torino and Department of Molecular Biotechnology and Health Sciences, University of Turin, Turin, Italy*

[10]*Institute of Haematology, Fondazione Policlinico Universitario A. Gemelli IRCCS, Rome, Italy*

[11]*Division of Hematology, Department of Translational Medicine, University of Eastern Piedmont, Novara, Italy*

[12]*Hematology and Stem Cell Transplantation Unit, Ospedale Oncologico A. Businco AO Brotzu, Cagliari, Italy*

[13]*Hematology Unit, Hematology and Oncology Department, Cosenza, Italy*

[14]*Hematology, Department of Medical Sciences, St. Anna University Hospital, Ferrara, Italy*

[15]*Department of Emergency and Organ Transplantation (D.E.T.O.), Hematology Section, University of Bari, Bari, Italy*

[16]*Hematology, Department of Biomedicine and Prevention, University Tor Vergata, Rome, Italy*

[17]*Department Hematology, Grande Ospedale Metropolitano, Reggio Calabria, Italy*

[18]*Hematology, Department of Translational and Precision Medicine, 'Sapienza' University, Rome, Italy*

Correspondence

Stefano Molica, Department of Hematology-Oncology, Azienda Ospedaliera Pugliese-Ciaccio, Viale Pio X, 88100 Catanzaro, Italy.

Email: smolica@libero.it

ORCID

Stefano Molica https://orcid.org/0000-0003-2795-6507

Andrea Visentin https://orcid.org/0000-0003-0271-7200

Gianluigi Reda https://orcid.org/0000-0003-4687-7089

Anna Maria Frustaci https://orcid.org/0000-0003-2587-7901

Luca Laurenti https://orcid.org/0000-0002-8327-1396

Riccardo Moia https://orcid.org/0000-0001-7393-1138

Marina Deodato https://orcid.org/0000-0003-0010-6107

Francesca Romana Mauro https://orcid.org/0000-0003-2425-9474

REFERENCES

1. Molica S, Seymour JF, Polliack A. A perspective on prognostic models in chronic lymphocytic leukemia in the era of targeted agents. *Hematol Oncol*. 2021;39(5):595-604.
2. Burger JA. Treatment of chronic lymphocytic leukemia. *N Engl J Med*. 2020;383(5):460-473.
3. Kittai AS, Miller C, Goldstein D, et al. The impact of increasing karyotypic complexity and evolution on survival in patients with CLL treated with ibrutinib. *Blood*. 2021;138(23):2372-2382.
4. Rigolin GM, Del Giudice I, Bardi A, et al. Complex karyotype in unfit patients with CLL treated with ibrutinib and rituximab: the GIMEMA LLC1114 phase 2 study. *Blood*. 2021;138(25):2727-2730.
5. International CLL-IPI Working Group. An international prognostic index for patients with chronic lymphocytic leukaemia (CLL-IPI): a meta-analysis of individual patient data. *Lancet Oncol*. 2016;17(6):779-790.
6. Delgado J, Doubek M, Baumann T, et al. Chronic lymphocytic leukemia: a prognostic model comprising only two biomarkers (IGHV mutational status and FISH cytogenetics) separates patients with different outcome and simplifies the CLL-IPI. *Am J Hematol*. 2017;92(4):375-380.
7. Kutsch N. CLL-IPI: valid in the era of oral inhibitors? *Blood*. 2021;138(2):106-107.
8. Hallek M, Al-Sawaf O. Chronic lymphocytic leukemia: 2022 update on diagnostic and therapeutic procedures. *Am J Hematol*. 2021;96(12):1679-1705.
9. Allan JN, Shanafelt T, Wiestner A, Moreno C, et al. Long-term efficacy of first-line ibrutinib treatment for chronic lymphocytic leukaemia in patients with TP53 aberrations: apooled analysis from four clinical trials. *Br J Haematol*. 2022;196(4):947-953.
10. Kipps TJ, Fraser G, Coutre SE, Brown JR, et al. Long-term studies assessing outcomes of Ibrutinib therapy in patients with Del(11q) chronic lymphocytic leukemia. *Clin Lymphoma Myeloma Leuk*. 2019;19(11):715-722.e6.
11. Soumerai JD, Ni A, Darif M, et al. Prognostic risk score for patients with relapsed or refractory chronic lymphocytic leukaemia treated with targeted therapies or chemoimmunotherapy: a retrospective, pooled cohort study with external validations. *Lancet Haematol*. 2019;6(7):e366-e374.
12. Ahn IE, Tian X, Ipe D, Cheng M, et al. Prediction of outcome in patients with chronic lymphocytic leukemia treated with ibrutinib: development and validation of a four-factor prognostic model. *J Clin Oncol*. 2021;39(6):576-585.
13. Ahn IE, Ruppert AJ, Wiestner A, et al. Performance of Standard Prognostic Models in Older Adults Receiving Ibrutinib for Treatment-Naïve (TN) Chronic Lymphocytic Leukemia (CLL): A Post Hoc Analysis of Alliance A041202 Phase 3 Trial. *Blood*. 2021;138(Supplement 1):2642a.

14. Visentin A, Mauro FR, Cibien F, et al. Continuous treatment with Ibrutinib in 100 untreated patients with TP53 disrupted chronic lymphocytic leukemia: a real-life campus CLL study. *Am J Hematol*. 2022;97(3):E95-E99.
15. Woyach JA, Ruppert AS, Heerema NA, et al. Ibrutinib regimens versus Chemoimmunotherapy in older patients with untreated CLL. *N Engl J Med*. 2018;379(26):2517-2528.

SUPPORTING INFORMATION

Additional supporting information may be found in the online version of the article at the publisher's website.

Received: 4 September 2021 | Revised: 7 February 2022 | Accepted: 10 February 2022

DOI: 10.1002/ajh.26509

Transient receptor potential channel vanilloid type 2 in red cells of cannabis consumer

To the Editor:

The abundance of the transient receptor potential channel vanilloid type 2 (TRPV2) in red blood cells (RBCs) was recently discovered,[1] inciting immediate discussion on its potential physiological importance.[2] TRPV2 is a reportedly mechanosensitive nonselective cation channel with numerous properties similar to those of Piezo1.[2] It has been proposed that TRPV2 may cause the induction of storage lesions in RBCs.[2,3] Furthermore, TRPV2 channels can be activated by cannabidiol or Δ9-tetrahydrocannabinol (Δ9-THC) and vice versa; thus, the changes induced in RBC by the application of Δ9-THC can be attributed to TRPV2 channel activity, which was first reported in RBCs of TRPV2-KO mice.[1]

Figure 1A,B shows confocal images of the RBCs of a 29-year-old man who participated in an initial study.[1] Under control conditions (HEPES-buffered solution), the RBCs were predominantly discocytes, as expected for healthy donors (Figure 1A). The addition of 30 μM Δ9-THC led to a large fraction of super-hydrated spherocytes (Figure 1B). Another representative healthy donor, under control conditions and with Δ9-THC stimulation, showed a significantly milder response, as depicted in Figure 1C,D, respectively. This was substantiated by the quantitative comparison of healthy controls (Figure 1E) with the proband under investigation (Figure 1F). The medical history of the donor revealed no significant findings other than regular cannabis consumption (smoking 2–3 g marijuana daily for several months).

Further studies were conducted in the proband and in two additional marijuana consumers with very similar smoking habits. Blood was collected to further investigate increased RBC sensitivity to Δ9-THC stimulation. First, we confirmed the initial result of the super-hydrated RBCs by comparing confocal images of the three male marijuana smokers (MS) with three age-matched male nonsmokers (NS) (35.7 ± 1.2 vs. 36.3 ± 6.4 years; $p = .9$), as outlined in Figure S1.

Next, we performed a complete RBC count, in the central clinical laboratory of Saarland University Hospital, to compare MS to NS. Based on the confocal recordings, we expected, but did not find, differences in the mean cellular volume (MCV) upon application of 30 μM Δ9-THC for all probands (Figure S2A). However, we found a slight MCV increase in the MS group compared with the NS group (Figure 1G), although, with a sample size of $N = 3$, this increase did not reach the $p < .05$ significance level. In contrast, the RBC distribution width (RDW) was significantly different between the MS and NS groups (Figure 1H). To explain the discrepancy between the confocal measurements and the RBC count, we identified experimental timing as a confounding parameter. While the cell swelling is a transient process that is undetectable after 45 min of acute Δ9-THC stimulation (-Figure S2B), this time limit passed within the routine handling at the central laboratory. Furthermore, clinical cell counters are optimized devices that provide accurate and reproducible measures, that is, the methodological contribution to the variations in the measurements was minimal and we are able to detect more subtle changes than with other methods for the steady-state conditions (Figure 1G,H). Additionally, the RBC Ca^{2+} response was investigated in terms of Fluo-4 fluorescence intensity with acute 30 μM Δ9-THC stimulation using flow cytometry (LSRFortessa, BD Biosciences, Franklin Lakes, NJ), and it showed an increase in the high Ca^{2+} RBC fraction upon Δ9-THC stimulation (Figure 1I,J).

Whether the heightened sensitivity of MS versus NS RBCs was caused by hypersensitizing TRPV2 or by modulation of its expression level during erythropoiesis was addressed by comparing MS and NS RBCs using functional patch-clamp measurements and western blotting. Figure 1K depicts a representative example of whole-cell RBCs currents of an MS that were measured in an automated patch-clamp robot (SynchroPatch 384, Nanion Technologies, Munich, Germany), both with and without 30 μM Δ9-THC application. Figure S3 shows the current changes of all responding cells, which were plotted separately for each proband. The average differential current (difference before and after Δ9-THC application) of the MS versus NS is plotted in Figure 1L. These numbers present the recordings at a clamped potential (−100 mV) and the cellular conductance under the experimental (artificial but highly reproducible) patch-clamp conditions, not reflecting the channel properties in intact RBCs at an unclamped membrane potential. This indicates a similar cellular conductance for MS and NS RBCs, and thus similarity in TRPV2 expression levels. Furthermore, the percentage of responding cells (Figure 1M) was in the same order of magnitude as the percentage of high Ca^{2+} cells outlined in Figure 1J. The western blots based on two different TRPV2 antibodies (Figure 1N,O and Figure S4) were consistent with the patch-clamp data, showing no significant differences in expression levels between MS and NS. Notably, unaltered TRPV2 expression levels in RBC suggest that TRPV2 expression regulation was likely not perturbed during erythropoiesis.

However, when compared with discocytes, the increased cross section and the decreased deformability of overhydrated RBCs are